Accepted Article

Rho Kinase (ROCK) collaborates with Pak to Regulate Actin Polymerization and Contraction in Airway Smooth Muscle

Wenwu Zhang, Bhupal P. Bhetwal and Susan J. Gunst

Dept. of Cellular & Integrative Physiology

Indiana University School of Medicine, Indianapolis, IN 46202.

Running Title: *ROCK regulates smooth muscle contraction by regulating actin polymerization*

Corresponding Author

Susan J. Gunst, PhD
Dept. of Cellular and Integrative Physiology
Indiana University School of Medicine
635 Barnhill Dr.
Indianapolis, IN 46202

ABSTRACT

Rho kinase (ROCK), a RhoA GTPase effector, can regulate the contraction of airway and other smooth muscle tissues. In some tissues, ROCK can inhibit myosin regulatory light chain (RLC) phosphatase, which increases the phosphorylation of myosin RLC and promotes smooth muscle contraction. ROCK can also regulate cell motility and migration by affecting F-actin dynamics. Actin polymerization is stimulated by contractile agonists in airway smooth muscle tissues and is required for contractile tension development in addition to myosin RLC phosphorylation. We investigated the mechanisms by which ROCK regulates the contractility of tracheal smooth muscle tissues by expressing a kinase inactive mutant of ROCK, ROCK-

_____

K121G, in the tissues or by treating them with the ROCK inhibitor, H-1152P. Our results show no role for ROCK in the regulation of non-muscle or smooth muscle myosin RLC phosphorylation during contractile stimulation in this tissue. We find that ROCK regulates airway smooth muscle contraction by mediating activation of the serine-threonine kinase, Pak, to promote actin polymerization. Pak catalyzes paxillin phosphorylation on Ser273 and coupling of the GIT1-βPIX-Pak signaling module to paxillin, which activates the GEF activity βPIX towards cdc42. Cdc42 is required for the activation of Neuronal Wiskott-Aldrich Syndrome protein (N-WASp), which transmits signals from cdc42 to the Arp2/3 complex for the nucleation of actin filaments. Our results demonstrate a novel molecular function for ROCK in the regulation of Pak and cdc42 activation that is critical for the processes of actin polymerization and contractility in airway smooth muscle.

KEY POINTS SUMMARY

- The mechanisms by which Rho kinase (ROCK) regulates airway smooth muscle contraction were determined in tracheal smooth muscle tissues. ROCK may mediate smooth muscle contraction by inhibiting myosin regulatory light chain (RLC) phosphatase. ROCK can also regulate F-actin dynamics during cell migration, and actin polymerization is critical for airway smooth muscle contraction.

- Our results show that ROCK does not regulate airway smooth muscle contraction by inhibiting myosin RLC phosphatase or by stimulating myosin RLC phosphorylation.

- We find that ROCK regulates airway smooth muscle contraction by activating the serine-threonine kinase Pak, which mediates the activation of Cdc42 and Neuronal-Wiskott-Aldrich Syndrome protein (N-WASp). N-WASP transmits signals from cdc42 to the Arp2/3 complex for the nucleation of actin filaments.

- These results demonstrate a novel molecular function for ROCK in the regulation of Pak and cdc42 activation that is critical for the processes of actin polymerization and contractility in airway smooth muscle.

2

INTRODUCTION

Rho-kinase (ROCK) is a serine threonine kinase that acts as a downstream effector of RhoA GTPase to regulate the contractility and motility of many cell and tissue types (Leung *et al.*, 1996; Matsui *et al.*, 1996; Somlyo & Somlyo, 2004; Liu *et al.*, 2006; Amin *et al.*, 2013). ROCK regulates the contractility of airway smooth muscle and has been proposed as a possible target for the treatment of asthma (Yoshii *et al.*, 1999; Gosens *et al.*, 2006; Liu *et al.*, 2006; Kume, 2008; Lan *et al.*, 2015). However, the mechanism by which ROCK regulates airway smooth muscle contractility is unclear.

In both smooth muscle and non-muscle cells and tissues, actomyosin crossbridge cycling is widely recognized as the primary mechanism for contraction and tension development. The activation of smooth muscle (SM) and non-muscle (NM) myosin is regulated by phosphorylation of myosin regulatory light chain (RLC) on Ser19 and Thr18 (Ikebe *et al.*, 1986). RhoA and ROCK have been shown to regulate phosphorylation of the RLC of myosin by inhibiting the catalytic activity of myosin RLC phosphatase or by directly phosphorylating myosin RLC (Amano *et al.*, 1996; Kimura *et al.*, 1996; Somlyo & Somlyo, 2003; Puetz *et al.*, 2009). Both ROCK and RhoA play an important role in regulating the contractility and shortening of vascular smooth muscle tissues, and there is evidence that this results from their role in the regulation of smooth muscle (SM) myosin RLC phosphorylation (Somlyo & Somlyo, 2003; Puetz *et al.*, 2009). However, in airway smooth muscle tissues, while the inhibition of RhoA activation profoundly depresses agonist-induced tension development, it has little effect on SM myosin II RLC phosphorylation (Zhang *et al.*, 2010; Zhang *et al.*, 2012; Zhang *et al.*, 2015). RhoA regulates the contractility of airway smooth muscle primarily by cytoskeletal mechanisms that are independent of SM myosin II RLC phosphorylation (Zhang *et al.*, 2010; Zhang *et al.*, 2012; Zhang & Gunst, 2017).

ROCK is also known to regulate cell motility and migration through effects on F-actin dynamics (Maekawa *et al.*, 1999; Worthylake & Burridge, 2003; Amano *et al.*, 2010; Guilluy *et al.*, 2011). Actin polymerization and cytoskeletal reorganization play a key role in the regulation of active tension development in airway smooth muscle and in other smooth muscle tissues (Herrera *et al.*, 2004; Corteling *et al.*, 2007; Rembold *et al.*, 2007; Gunst & Zhang, 2008; Kim *et al.*, 2008; Hill & Meininger, 2012; Walsh & Cole, 2013; Zhang *et al.*, 2015; Hill & Meininger, 2016; Hong *et al.*, 2016). In airway smooth muscle, the inhibition of actin polymerization depresses tension development in response to contractile stimulation

3

with little or no effect on SM myosin II RLC chain phosphorylation and crossbridge cycling (Mehta & Gunst, 1999; Zhang *et al.*, 2005; Gunst & Zhang, 2008). Agonist-stimulated actin polymerization requires activation of the actin filament nucleation promoting protein, N-WASp (neuronal Wiskott-Aldrich syndrome protein) (Zhang *et al.*, 2005). N-WASp activation is directly regulated by the small GTPase, cdc42. Activated cdc42 catalyzes a conformational change in N-WASp that enables it to couple to the Arp2/3 complex, which forms a template for actin polymerization (Rohatgi *et al.*, 1999; Higgs & Pollard, 2000; Rohatgi *et al.*, 2000). cdc42 is activated during the contractile stimulation of airway smooth muscle tissues, and cdc42 activation is necessary for N-WASp activation, actin polymerization and active tension development in this tissue (Tang & Gunst, 2004).

The contractile stimulation of airway smooth muscle induces the recruitment of proteins to membrane-associated integrin adhesion junctions (adhesomes) via a RhoA-dependent mechanism mediated by non-muscle (NM) myosin II (Zhang *et al.*, 2012; Zhang *et al.*, 2015; Zhang & Gunst, 2017). RhoA regulates the formation and activation of submembranous NM myosin II filaments that catalyze the movement of inactive cytoskeletal proteins to the membrane, where they are assembled into adhesome signaling complexes that regulate cytoskeletal processes. Paxillin, vinculin and focal adhesion kinase (FAK) are all recruited to adhesome complexes by RhoA-activated NM myosin II filaments. RhoA-mediated NM myosin II activation and adhesome signaling complex assembly are essential steps in excitation-contraction coupling and tension development in airway smooth muscle tissues during agonist-induced contractile activation; however it is not known whether ROCK acts as a downstream effector in these RhoA-mediated processes.

In the current study, we sought to determine the molecular mechanisms by which ROCK contributes to the contractile activation of airway smooth muscle. Our results suggest a novel molecular function for ROCK in adhesome signaling processes that regulate actin polymerization during the contractile activation of airway smooth muscle. Our study demonstrates a unique role for ROCK that is distinct from its well-known role in the regulation of myosin RLC phosphorylation.

METHODS

Ethical Approval. All procedures were in accordance with procedures approved by the Institutional Animal Care and Use Committee (IUCAC) of Indiana University School of Medicine under the National Research Council's Guide for the Care and Use of Laboratory

4

Animals. Mongrel dogs (20-25 kg, any gender) were procured by the Indiana University Laboratory Animal Resource Center (LARC) at Indiana University School of Medicine from LBL Kennels, Reelsville, Indiana. Animals were euthanized by LARC personnel in accordance with procedures approved by the Institutional Animal Care and Use Committee (IUCAC) of Indiana University School of Medicine by IV injection of Fetal Plus (pentobarbital sodium 390 mg/ml; propylene glycol, 0.01 mg/ml; ethyl alcohol; 0.29 mg/ml; benzyl alcohol (preservative), 0.2 mg/ml) at a dose of approximately 0.3ml/kg. After euthanization, a tracheal segment was immediately removed by laboratory personnel and placed in physiological saline solution (PSS). All investigators understand the ethical principles under which the Journal of Physiology operates and all work complies with these principles.

Preparation of smooth muscle tissues and measurement of force. A tracheal segment was immersed in physiological saline solution (PSS) (composition in mM: 110 NaCl, 3.4 KCl, 2.4 CaCl$_2$, 0.8 MgSO$_4$, 25.8 NaHCO$_3$, 1.2 KH$_2$PO$_4$, and 5.6 glucose, bubbled with 95% O$_2$ and 5% CO$_2$) immediately after removal. Tracheal smooth muscle was then dissected free of connective and epithelial tissues and cut into narrow strips (1.0 x 0.2-0.5 x 15 mm). Tissue strips were then mounted in a tissue bath in PSS at 37ºC and attached to Grass force-displacement transducers. Prior to the beginning of each experimental protocol, muscle length was increased to maintain a preload of approximately 0.5-1.0g, and tissues were stimulated repeatedly with 10^{-5} M ACh until stable contractile responses were obtained. The force of contraction in response to ACh was determined before and after treatment with plasmids or other reagents.

Immunoblots. At the end of each protocol, muscle tissues were rapidly frozen in liquid N$_2$ and pulverized using a mortar and pestle. Pulverized muscle tissues were mixed with extraction buffer containing: 20 mM Tris-HCl at pH 7.4, 2% Triton X-100, 0.4% SDS, 2 mM EDTA, phosphatase inhibitors (2 mM sodium orthovanadate, 2 mM molybdate, and 2 mM sodium pyrophosphate), and protease inhibitors (2 mM benzamidine, 0.5 mM aprotinin, and 1 mM phenylmethylsulfonyl fluoride). Each sample was centrifuged, and the supernatant was then boiled in sample buffer (1.5% dithiothreitol, 2% SDS, 80 mM Tris-HCl, pH 6.8, 10% glycerol, and 0.01% bromphenol blue) for 5 min. Proteins were separated by SDS-PAGE and transferred to nitrocellulose. The nitrocellulose membrane was blocked with 2-5% milk or LiCor blocking buffer for 1 h and probed with primary antibodies against proteins of interest

overnight followed by secondary antibodies for 1 h. Proteins were visualized by enhanced chemiluminescence (ECL) using a Bio-Rad ChemiDoc XRS detection system or by infrared fluorescence using a LiCor Odyssey imager.

Measurement of myosin RLC phosphorylation. Myosin light chain phosphorylation was analyzed by a modification of the method of Hathaway and Haeberle as previously described (Hathaway & Haeberle, 1985;Zhang *et al.*, 2005;Zhang *et al.*, 2010) Frozen muscle strips were immersed in dry ice precooled in acetone containing 10% w/v trichloroacetic acid and 10mM dithiothreitol. Proteins were extracted in 8 M urea, 20 mM Tris base, 22 mM glycine and 10 mM dithiothreitol. Phosphorylated and unphosphorylated myosin light chains were separated by glycerol-urea polyacrylamide gel electrophoresis, transferred to nitrocellulose then immunoblotted for myosin RLC. Myosin RLC phosphorylation was calculated as the ratio of phosphorylated myosin RLC to total RLC.

Two-dimensional electrophoresis for the analysis of NM and SM myosin RLC phosphorylation. The phosphorylation of SM and NM RLC chains was analyzed in tracheal smooth muscle extracts by 2-D electrophoresis as previously described (Zhang & Gunst, 2017) Canine tracheal smooth muscle tissues were stimulated with 10^{-5} M ACh or left unstimulated for 5 minutes and frozen in liquid nitrogen. Frozen muscle strips were immersed in dry ice-precooled acetone containing 10% (wt/vol) trichloroacetic acid and 10 mM DTT. Proteins were extracted in 7 M urea, 2 M thiourea, 2% (wt/vol) 3-[(3-cholamidopropyl) dimethylammonio]-1-propanesulfonate (CHAPS), 1% 3.9–5.1 immobilized pH gradient (IPG) buffer, and Roche complete protease inhibitor. Suitable amounts of sample were resolved in the first dimension using the acidic half of 17 cm pH 3.9-5.1 IPG dry strip gels. After separation in the first dimension, proteins were equilibrated in 6 M urea, 50 mM pH 6.4 Bis-Tris, 30% (vol/vol) glycerol, 2% SDS, 0.002% bromophenol blue, first containing 10 mM DTT and then containing 2.5% (wt/vol) iodoacetamide. Proteins were then separated in the second dimension by SDS-PAGE, transferred to nitrocellulose, then immunoblotted for total myosin RLC. Phosphorylation was calculated from densitometric and mass spectrometry analysis of the myosin RLC spots as previously described (Zhang & Gunst, 2017). The two less acidic spots (Spots 1 and 2) consist of unphosphorylated SM myosin RLC (Spot 1) and Ser19-phosphorylated SM myosin RLC (Spot 2). The two more acidic spots (Spots 3 and 4) contained unphosphorylated NM myosin RLC (Spot 3) and Ser19-phosphorylated NM myosin RLCs (Spot 4). However, di-phosphorylated (Thr18 and Ser19)

SM myosin RLC is present in extracts from stimulated smooth muscle tissues and was found to co-migrate with unphosphorylated NM myosin RLC (Spot 3). The proportion of NM myosin RLC to total RLC was determined from the density of the spots representing NM myosin RLCs (Spots 3 and 4) to the total myosin RLCs (Spots 1-4) from immunoblots from unstimulated smooth muscle tissues. The effect of ACh stimulation on the phosphorylation of NM myosin RLC was quantified based on the density of the phosphorylated NM myosin RLC (Spot 4) relative to the proportion of NM myosin RLC to SM myosin RLC.

Triton solubility assay. A Triton solubility assay was performed on extracts of smooth muscle tissues to separate cytoskeletal and Triton-soluble proteins (Zhang & Gunst, 2017). In brief, frozen and pulverized tracheal smooth muscle tissue samples were mixed with Triton X-100 lysis buffer (150 mM KCl, 20 mM PIPES, 10 mM Imidazole, pH 7.0, 0.05% Triton X-100, 1 mM $MgCl_2$, 1 mM EGTA, 1 mM DTT, 0.1 mM PMSF, 5 μg/ml aprotinin, 5 μg/mL leupeptin, 2 μg/mL pepstatin A, 1 mM Na_3VO_4, and 20 mM β-glycerophosphate) at 4° C. After 5 min, the lysates were centrifuged at 8,000 g for 5 min at 4°C, and the supernatant was removed as the soluble fraction. The pellet, the insoluble fraction, was added to equal volumes of Triton X-100 lysis buffer with additional 0.8% SDS and 2 mM EDTA, boiled for 5 min and rotated for 1 hour and then centrifuged at 16,000 g for 15 min at 4°C. The supernatant was transferred to another tube as the insoluble fraction. Equal volumes of soluble and insoluble fractions from the same sample were used for immunoblots.

Analysis of F-actin and G-actin. The relative proportions of F-actin and G-actin in smooth muscle tissues were analyzed as previously described (Zhang *et al.*, 2005; Zhang *et al.*, 2010; Zhang *et al.*, 2012). Briefly, each muscle strip was homogenized in 200 μl of F-actin stabilization buffer (50 mM PIPES, pH 6.9, 50 mM NaCl, 5 mM $MgCl_2$, 5 mM EGTA, 5% Glycerol, 0.1% Triton X-100, 0.1% Nonidet P-40, 0.1% Tween-20, 0.1% β-mercaptoethanol, 0.001% antifoam, 1 mM ATP, 1 μg/ml pepstatin, 1 μg/ml leupeptin, 10 μg/ml benzamidine, and 500 μg/ml tosyl arginine methyl ester). Supernatants of the protein extracts were collected after centrifugation at 150,000 *g* for 60 min at 37° C. The pellets were resuspended in 200 μl of ice-water containing 10 μM cytochalasin D and then incubated for 1 h and gently mixed every 15 min to depolymerize F-actin. The amount of actin in the supernatant (G-actin) and pellet (F-actin) fractions was then analyzed by immunoblot, and the ratios of F-actin to G-actin were determined using densitometry.

Transfection of smooth muscle tissues. Plasmids encoding wild type human ROCK and kinase inactive human ROCK, ROCK K121G, were introduced into tracheal smooth muscle strips by the method of reversible permeabilization as previously described (Tang *et al.*, 2003; Zhang *et al.*, 2005; Zhang *et al.*, 2010; Zhang *et al.*, 2012; Zhang *et al.*, 2016; Zhang & Gunst, 2017). Muscle tissues were attached to metal mounts to maintain them at constant length, and then incubated successively in each of the following solutions: *Solution 1* (at 4º C for 120 min) containing (in mM): 10 EGTA, 5 Na_2ATP, 120 KCl, 2 $MgCl_2$, and 20 N-tris (hydroxymethyl) methyl-2-aminoethanesulfonic acid (TES); *Solution 2* (at 4º C overnight) containing (in mM): 0.1 EGTA, 5 Na_2ATP, 120 KCl, 2 $MgCl_2$, 20 TES, and 20 µg/ml plasmids. *Solution 3* (at 4º C for 30 min) containing (in mM): 0.1 EGTA, 5 Na_2ATP, 120 KCl, 10 $MgCl_2$, 20 TES; and *Solution* 4 (at 22º C for 90 min) containing (in mM): 110 NaCl, 3.4 KCl, $0.8MgSO_4$, 25.8 $NaHCO_3$, 1.2 KH_2PO_4, and 5.6 dextrose. *Solutions 1-3* were maintained at pH 7.1 and aerated with 100% O_2. *Solution 4* was maintained at pH 7.4 and was aerated with 95% O_2-5% CO_2. After 30 min in *Solution 4*, $CaCl_2$ was added gradually to reach a final concentration of 2.4 mM. The strips were then placed in serum-free DMEM containing 5mM Na_2ATP, 100 U/ml penicillin, 100 µg/ml streptomycin, 50 µg/ml Kanamycin, 2.5 µg/ml antifungal, and 20 µg/ml plasmids and incubated in a CO_2 incubator at 37ºC for 2 days to allow for the expression of recombinant proteins. The expression levels of the WT ROCK and ROCK K121G in transfected muscle tissues was quantitated from immunoblots and found to average about 50% of the level of the endogenous ROCK (Fig. 1B).

Immunoprecipitation of Proteins. Pulverized muscle tissues were mixed with lysis buffer (1% Np-40, 20 mM Tris·HCl (pH 7.6), 0.3% NaCl, 10% glycerol, 2 mM EDTA, phosphatase inhibitors (in mM: 2 sodium orthovanadate, 2 molybdate, and 2 sodium pyrophosphate), and protease inhibitors (in mM: 2 benzamidine, 0.5 aprotinin, and 1 phenylmethylsulfonyl fluoride) for 2 h. Each sample was centrifuged (14,000 *g*) for the collection of supernatant. Muscle extracts containing equal amounts of protein (800-1200 µg) were precleared for 30 min with 30 µl of 10% protein A/G-Sepharose and then incubated overnight with primary antibodies. Samples were then incubated for 2 h with 40 µl of a 10% suspension of protein A/G-Sepharose beads. Immunocomplexes were washed three times in a buffer containing 50 mM Tris-HCl, pH 7.6, 150 mM NaCl, and 0.1% Triton X-100. All procedures of immunoprecipitation were performed at 4°C. The immunoprecipitates were separated by

SDS-PAGE followed by transfer to nitrocellulose membranes. Proteins were quantitated by scanning densitometry.

*Assessment of cdc42 activatio*n. The activation of cdc42 was determined using a pull-down assay for activated cdc42 (Tang & Gunst, 2004;Zhang *et al.*, 2012). Pulverized muscle tissues were mixed with lysis buffer (see *Immunoprecipitation of Proteins* for details) for 2 hours at 4º C. The extracted proteins were reacted with GST-Pak Binding Domain. Activated GTP-bound cdc42 was affinity-precipitated by glutathione beads and quantified by immunoblot.

Cell dissociation. Freshly dissociated primary tracheal smooth muscle cells were used for cell imaging protocols to avoid the morphologic and phenotypic changes that occur with the extended culture of smooth muscle cells (Opazo Saez *et al.*, 2004; Zhang *et al.*, 2005; Zhang *et al.*, 2012). Tracheal muscle strips were minced and transferred to 5 ml of dissociation solution (in mM: 130 NaCl, 5 KCl, 1.0 CaCl2, 1.0 MgCl2, 10 HEPES, 0.25 EDTA, 10 D-glucose, and 10 taurine, pH 7.0) with collagenase (type IV, 400 U/ml), papain (type IV, 30 U/ml), bovine serum albumin (1 mg/ml), and dithiothreitol (DTT; 1 mM) and placed in a 37°C shaking water bath at 60 oscillations/min for 15-20 min. They were then washed with a Hepes-buffered saline solution (in mM: 130 NaCl, 5 KCl, 1.0 $CaCl_2$, 1.0 $MgCl_2$, 20 HEPES, and 10 D-glucose, pH 7.4) and triturated with a pipette to dissociate individual smooth muscle cells. The solution of dissociated cells was poured onto glass coverslips. The cells were allowed to adhere to the coverslips for 30-60 minutes at room temperature and then stimulated with ACh (10^{-5} M) for 5 min at 37°C or not stimulated. Stimulated and unstimulated cells were fixed for 10 min in 4% paraformaldehyde (vol/vol) in phosphate-buffered saline (in mM: 137 NaCl, 4.3 Na_2HPO_4, 1.4 KH_2PO_4, and 2.7 KCl, pH 7.4).

In Situ Proximity Ligation Assay. In situ proximity ligation assays (PLA) (Soderberg *et al.*, 2006;Soderberg *et al.*, 2008) were performed to detect protein interactions in dissociated tracheal smooth muscle cells as previously described (Huang *et al.*, 2011; Zhang *et al.*, 2012; Zhang *et al.*, 2016; Zhang & Gunst, 2017). Target proteins were reacted with primary antibodies raised in different species, and a pair of oligonucleotide-labeled secondary antibodies conjugated to + and − PLA probes were targeted to each pair of primary antibodies. When the probes are bound in very close proximity (<40 nm), they form circular DNA strands that serve as templates for localized rolling circle amplification, resulting in a

fluorescent signal (spot) that enables individual interacting pairs of the target protein molecules to be visualized. The PLA signal thus enables the detection of a complex between two target proteins at a very high resolution. Protein interactions in each cell were evaluated by visualizing PLA fluorescent spots using a Zeiss LSM 510 confocal microscope. Interactions between specific proteins were quantified by assessing the total number of PLA fluorescent spots for each cell using Olink Bioscience Image Tools software.

Reagents and antibodies. The ROCK inhibitor, H-1152P, was obtained from Sigma Chemical Co. H-1152P inhibits the kinase activity of ROCK1 and ROCK2 by blocking the ATP binding site in the kinase domain (Ikenoya *et al.*, 2002). The Duolink^{TM} *in situ* proximity ligation assay (Olink Bioscience) was obtained from Sigma Chemical Co. Cdc42 activation assay kits were obtained from Cytoskeleton (Denver, CO). All other chemical reagents were obtained from Sigma Chemical Co.

Plasmids encoding wild type human ROCK and kinase inactive human ROCK, ROCK K121G (Oude Weernink *et al.*, 2000; Croft *et al.*, 2004), were generously provided by Dr. K. Kaibuchi of Nagoya University, Japan. The kinase-inactive mutant (ROCK K121G) was created by changing lysine 121 to glycine. Escherichia coli (Bluescript) transformed with these plasmids were grown in LB medium, and plasmids were purified by alkaline lysis with SDS using a purification kit from Qiagen Inc.

Sources of antibodies are as follows: monoclonal mouse anti-human paxillin (Cat #610569, BD Biosciences); polyclonal rabbit anti-human paxillin phospho-tyrosine 118 (Cat #44-722G, Invitrogen); polyclonal rabbit anti-human paxillin phospho-serine 273 (Cat #44-1028G, Invitrogen); mouse monoclonal anti-human talin (Cat #T3287, Sigma-Aldrich); polyclonal rabbit anti-human ROCK1 (Cat #4035T, Cell Signaling); polyclonal rabbit anti-human Pak1 (Cat #2602, Cell Signaling); polyclonal rabbit anti-human phospho-Pak Thr 423/402 (Cat #2601, Cell Signaling); polyclonal rabbit anti-human GIT1 (Cat #2909, Cell Signaling); mouse monoclonal anti-human N-WASp (Cat #4848 Cell Signaling); polyclonal rabbit anti-human N-WASp phospho-tyrosine 256 (Cat #ab23395 Abcam); monoclonal mouse anti-human cdc42 (Cat #610929, BD Biosciences); horseradish peroxidase-conjugated IgG (Cat # NA931 & NA934 Amersham Biosciences); Mouse monoclonal anti-human MYPT1 (Cat #612164 BD Biosciences); monoclonal mouse anti-actin [clone AC-40; Sigma), used at 1:10,000 dilution]; monoclonal mouse anti-human myosin IIA (Cat #ab55456, Abcam); polyclonal rabbit anti-human non-muscle myosin IIB (Cat #M7939, Sigma);

monoclonal mouse anti myc-tag (Cat #2276 (9B11) Cell Signaling); IRDye® 680RD Donkey-anti-Mouse Antibody (Cat #926-68070) and IRDye® 800CW Donkey-anti-Rabbit Antibody (Cat #925-32211, LiCor Biosciences). Polyclonal rabbit vinculin antibody (against canine cardiac vinculin) and polyclonal rabbit myosin RLC antibody were custom made by BABCO (Richmond, CA). Primary antibodies were diluted at 1:1000 for immunoblotting unless otherwise indicated.

All antibodies have been validated to confirm their reaction with the designated antigen in the smooth muscle tissue extracts, immunoblots, or fixed cells in the present or in previous studies (Huang *et al.*, 2011; Zhang *et al.*, 2012; Zhang *et al.*, 2016; Zhang & Gunst, 2017).

Statistical analysis. Comparisons between two groups were performed using paired or unpaired two-tailed Student's t tests. Values refer to the number of cells or tissue strips used to obtain mean values. $p < 0.05$ was considered statistically significant.

RESULTS

ROCK regulates acetylcholine (ACh) induced contractile force but not myosin RLC phosphorylation in tracheal smooth muscle tissues. We assessed the role of ROCK in ACh-induced myosin RLC phosphorylation and tension development in canine tracheal smooth muscle tissues by inhibiting ROCK activation using a kinase inactive ROCK mutant, C-myc-ROCK1 K121G, and a small molecule ROCK inhibitor, H-1152. Tracheal smooth muscle tissues were transfected with plasmids encoding C-myc-ROCK1 K121G or wild type (WT) ROCK1 by reversible permeabilization. Tissues were then incubated for 2 days to allow for expression of the recombinant proteins. Alternatively, tracheal smooth muscle tissues were incubated with 10^{-6} M H-1152P for 30 min to inhibit ROCK. Contractile force was measured in each tissue before and after ROCK inhibition (Fig.1A). The inhibition of ROCK activity suppressed force development by more than 50% (ROCK K121G, 43±2.5% of Sham (n=7, p<0.05); H-1152, 44±7.7% of Untreated (n=7, p<0.05) (Fig. 1A). The expression of myc-ROCK1 K121G in transfected tissues was confirmed by immunoblot against the myc epitope (Fig 1B).

The inhibition of ROCK activity by H-1152P or ROCK1 K121G in the airway smooth muscle tissues was confirmed by measuring their effect on Thr853 phosphorylation

11

of the ROCK substrate, MYPT1, in response to 10^{-5} M ACh (Khromov et al., 2009). As ROCK is the only kinase that can phosphorylate MYPT at Thr853, phosphorylation at this site is used as an indicator of cellular ROCK activity (Grassie *et al.*, 2011; Eto & Kitazawa, 2017). The phosphorylation of MYPT1 on Thr853 increased in response to stimulation of the tissues with ACh in untreated and in Sham-treated tissues. The increase in Thr853 phosphorylation in response to ACh was completely inhibited by the expression of ROCK K121G or by treatment of the tissues with H-1152P (Fig. 1B,C).

The phosphorylation of MYPT1 by ROCK can inactivate myosin light chain phosphatase, thus promoting myosin RLC phosphorylation and tension development in some smooth muscle tissue types (Khromov *et al.*, 2009; Eto & Kitazawa, 2017). We therefore assessed the effect of ROCK inhibition on the regulation of ACh induced myosin RLC phosphorylation in tracheal smooth muscle tissues (Fig 1D). The inhibition of ROCK by the expression of ROCK K121G or by H-1152P in tracheal smooth muscle tissues had no significant effect on myosin RLC phosphorylation in response to stimulation with ACh. Thus, ROCK does not regulate tension development in airway smooth muscle by regulating myosin RLC phosphorylation.

ROCK regulates actin polymerization in response to ACh stimulation of smooth muscle tissues. We evaluated the role of ROCK in regulating ACh-induced actin polymerization in airway smooth muscle using a fractionation assay to assess the ratio of F- to G-actin in each tissue after 5 min stimulation with 10^{-5} M ACh. ROCK was inhibited using 1 μM H-1152P or by expressing ROCK K121G in the tissues. ACh induced significant increases in the ratio of F-actin to G-actin in the sham-treated tissues and in tissues expressing WT ROCK (Fig.2). The expression of ROCK K121G completely inhibited the increase in actin polymerization. The ACh induced increase in the ratio of F-actin to G-actin was also completely inhibited by the pretreatment of tissues with ROCK inhibitor, H-1152P.

ROCK does not regulate NM myosin activation during contractile stimulation of airway smooth muscle. Contractile stimulation triggers the assembly and activation of NM myosin filaments at the cortex of the cell. Cortical NM myosin filaments catalyze the recruitment of adhesome proteins to membrane adhesion junctions (Zhang & Gunst, 2017). In airway smooth muscle, NM myosin filament assembly and activation is catalyzed by the small GTPase RhoA (Zhang & Gunst, 2017). RhoA inactivation inhibits NM myosin filament assembly and the phosphorylation of the NM myosin RLC, but it has no effect on SM RLC

12

phosphorylation (Zhang & Gunst, 2017). We therefore evaluated the possibility that ROCK acts as a downstream effector of RhoA in regulating the assembly and/or activation of NM myosin II in airway smooth muscle.

We used 2-D gel electrophoresis to separate NM and SM RLCs and analyze the effect of ROCK inhibition on NM myosin RLC phosphorylation in response to stimulation with ACh (Zhang & Gunst, 2017) (Fig. 3A). ROCK was inhibited by expressing ROCK1 K121G in the tissues. There was no significant difference in NM myosin RLC phosphorylation between tissues treated with ROCK1 K121G and Sham-treated tissues, although force was markedly depressed in the tissues expressing ROCK1 K121G.

We also evaluated the effect of ROCK inhibition on NM myosin filament assembly. NM myosin filament formation was determined by quantifying the ratio of NM myosin in the cytoskeletal and Triton X-soluble fractions of tracheal tissue extracts (Zhang & Gunst, 2017). The proportion of NM myosin IIA in the cytoskeletal fraction of smooth muscle tissue extracts increased similarly after stimulation with ACh whether or not ROCK was inhibited (Figure 3B).

In situ PLA analysis was also used to assess NM myosin filament formation by evaluating interactions between A and B isoforms of NM myosin II. NM myosin II isoforms can co-assemble into heterotypic filaments (Beach *et al.*, 2014; Beach & Hammer, 2015), therefore the formation of NM myosin II polymers can be quantified by assessing interactions between NM myosin IIA and IIB isoforms (Zhang & Gunst, 2017). Stimulation with ACh increased the interaction of NM myosin IIA and IIB isoforms dramatically in cells stimulated with ACh whether or not ROCK was inhibited (Fig 3C). These results demonstrate that ROCK does not act downstream of RhoA to regulate the assembly or activation of NM myosin filaments in airway smooth muscle.

ROCK does not regulate the assembly of adhesome complexes during the contractile stimulation of airway smooth muscle. Adhesome proteins are recruited to the membrane and are assembled into signaling complexes in response to the contractile stimulation of airway smooth muscle (Zhang & Gunst, 2008; Zhang *et al.*, 2012; Zhang *et al.*, 2015; Zhang *et al.*, 2016; Zhang & Gunst, 2017). Vinculin is recruited to the membrane bound in an inactive complex with paxillin (Huang *et al.*, 2011; Zhang *et al.*, 2012; Huang *et al.*, 2014). At the cell membrane, vinculin binds to talin and undergoes activation, forming a scaffold for the assembly of cytoskeletal signaling modules. The assembly of adhesome

signaling complexes in response to the contractile stimulation is mediated by NM myosin and is dependent on activation of the small GTPase RhoA (Zhang *et al.*, 2015; Zhang & Gunst, 2017).

We investigated the possible role of ROCK as an effector of the RhoA-mediated recruitment of cytoskeletal proteins to adhesome complexes. ROCK was inhibited in airway smooth muscle tissues by treating them with H-1152P. Airway smooth muscle cells were dissociated from airway smooth muscle tissues and *in situ* PLA was used to evaluate the role of ROCK in the recruitment of vinculin-paxillin complexes to the membrane in response to stimulation with ACh (Fig.4A). Paxillin-vinculin complexes were distributed throughout the cytoplasm in unstimulated cells. Stimulation of the cells with ACh resulted in the redistribution of paxillin-vinculin complexes to the membrane in untreated cells and in cells treated with H1152P; thus ROCK inhibition had no effect on the recruitment of paxillin-vinculin complexes to the membrane. A similar approach was used to evaluate the effect of ROCK inhibition on the interaction of vinculin with talin (Fig 4B). Very few talin-vinculin complexes were observed in unstimulated cells, indicating little interaction between vinculin and talin. Stimulation with ACh caused a dramatic increase in the number of PLA spots at the cell membrane, indicating the binding of vinculin to talin in membrane complexes. ROCK inhibition had no effect on the interaction of vinculin with talin in response to ACh. Thus, we conclude that ROCK is not an effector in RhoA-mediated adhesome assembly stimulated by ACh in airway smooth muscle tissues.

ROCK regulates the phosphorylation of paxillin on Ser273 and its coupling to the GIT1-βPIX-Pak complex in response to ACh stimulation in airway smooth muscle tissues. The stimulation of airway smooth muscle tissues catalyzes the phosphorylation of paxillin on Tyr31 and Tyr118, which regulates the coupling of N-WASp to paxillin via the adaptor protein Crk II (Tang *et al.*, 2005). Airway smooth muscle stimulation by ACh also catalyzes the phosphorylation of paxillin on Ser273 by Pak, which is a component of the highly conserved GIT1-βPIX-Pak signaling module (G-protein-coupled receptor kinase-interacting protein (GIT1), p21 activated kinase (Pak), and Pak interactive exchange factor (PIX) (Frank & Hansen, 2008; Zhang *et al.*, 2016). Paxillin Ser273 phosphorylation promotes the binding of paxillin to GIT1 within the GIT1-βPIX-Pak signaling module. The GEF activity of βPIX can then regulate the activation of cdc42 leading to the activation of N-WASp. Thus, paxillin Ser273 phosphorylation by Pak facilitates cdc42 activation through the GEF activity of βPIX within the GIT-βPIX-Pak complex. Paxillin is therefore a key mediator

in the formation of an adhesome signaling module that regulates cdc42 and N-WASp activation in response to contractile stimuli.

We evaluated the role of ROCK in the regulation of paxillin phosphorylation on Ser273 and on Tyr118 residues in response to contractile stimulation. ROCK was inhibited by treating muscle tissues with H-1152P or by expressing ROCK K121G. Stimulation of tracheal muscle tissues with 10^{-5}M ACh caused a significant increase in paxillin phosphorylation on Ser273 as well as on Tyr118 (Fig. 5A,B). Expression of ROCK K121G or treatment with H-1152P significantly inhibited the increase in paxillin Ser273 phosphorylation in response to ACh stimulation, but it had no effect on the ACh-stimulated increase in paxillin Tyr118 phosphorylation (Fig. 5A, B).

In situ proximity ligation assays (PLA) were performed on freshly dissociated tracheal smooth muscle cells to evaluate the interaction between paxillin and GIT1 (Fig. 6A, B). Very few spots were observed in unstimulated cells, indicating little interaction between paxillin and GIT1. Stimulation with ACh caused a dramatic increase in the number of PLA spots at the cell membrane, indicating an interaction of GIT1 with paxillin in membrane complexes. Very few spots were observed in ACh-stimulated cells dissociated from tissues treated with the ROCK K121G mutant or in ACh stimulated cells treated with H-1152P, indicating ROCK inhibition prevented the coupling of paxillin to GIT1 (Fig. 6A, B). These results demonstrate that ROCK regulates the interaction of the GIT1-βPIX-Pak signaling module with paxillin at membrane adhesome complexes by regulating the phosphorylation of paxillin on Ser273.

ROCK regulates the activation of Pak in response to ACh stimulation in airway smooth muscle tissues. The activation of Pak requires its autophosphorylation on Thr423 (Yu *et al.*, 1998; Zenke *et al.*, 1999). We evaluated the role of ROCK in the regulation of Pak activation by measuring Pak Thr423 phosphorylation in tissues in which ROCK activation was inhibited by expressing ROCK K121G or by treating them with H-1152P (Fig. 7A). ROCK inactivation significantly inhibited the increase in Pak Thr423 phosphorylation in response to ACh stimulation. To determine whether ROCK associates with Pak in airway smooth muscle tissues, Pak1 was immunoprecipitated from smooth muscle tissue extracts and Pak immunocomplexes immunoblotted for ROCK, or ROCK1 was immunoprecipitated and immunocomplexes immunoblotted for Pak (Fig.7B). ROCK was not detected in Pak immunocomplexes or ROCK immunocomplexes from unstimulated tissues; however, in immunocomplexes from ACh-stimulated tissues, ROCK was detected in Pak

immunocomplexes and Pak was detected in ROCK immunocomplexes. The interaction between ROCK and Pak induced by ACh stimulation was inhibited by the treatment of smooth muscle tissues with H-1152P (Fig. 7B). These results suggest that ROCK activity is necessary for the activation of Pak, and that ROCK thereby regulates the Ser273 phosphorylation of paxillin. Thus, our results demonstrate that the activation of ROCK is required for the coupling of the GIT1-βPIX-Pak signaling module to paxillin in airway smooth muscle.

Paxillin Ser273 phosphorylation and coupling of the GIT1-βPIX-Pak signaling module to paxillin is prerequisite to the activation of cdc42 in response to stimulation with ACh (Frank & Hansen, 2008; Zhang *et al.*, 2016). We analyzed the role of ROCK in the regulation of cdc42 activation in tracheal smooth muscle tissues using a pull-down assay for activated cdc42 (cdc42-GTP) (Tang & Gunst, 2004; Zhang *et al.*, 2012; Zhang *et al.*, 2016). The inactivation of ROCK by the expression of ROCK K121G or by treatment of the tissues with H-1152P resulted in the inhibition of cdc42 activation (Fig. 8A).

The actin polymerization initiator N-WASp must be phosphorylated on Tyr256 to undergo activation (Wu *et al.*, 2004; Zhang *et al.*, 2012). We evaluated the effect of ROCK inhibition on N-WASp activation in response to ACh by measuring its effect on N-WASp phosphorylation on Tyr256. ACh stimulation increased N-WASp phosphorylation on Tyr256 in the sham-treated and untreated tracheal smooth muscle tissues. The expression of ROCK K121G or treatment of the tissues with H-1152P completely inhibited the ACh-induced increase in N-WASp Tyr256 phosphorylation (Fig. 8B). These results suggest that ROCK regulates tension generation in airway smooth muscle by regulating signaling processes that mediate the activation of N-WASp and actin polymerization.

Thus, ROCK activation is required for the activation of cdc42, which regulates N-WASp activation and actin polymerization. These results demonstrate a unique role for ROCK in the regulation of airway smooth muscle contraction.

DISCUSSION

The development of contractile tension in airway smooth muscle depends on the activation of cytoskeletal processes involving actin polymerization and cytoskeletal reorganization as well as myosin RLC phosphorylation and crossbridge cycling (Mehta & Gunst, 1999; Zhang & Gunst, 2008; Zhang *et al.*, 2010). Our studies demonstrate that ROCK

plays a unique role in activating cytoskeletal signaling processes that lead to the polymerization of actin and the contraction of airway smooth muscle (Fig. 9). We find no role for ROCK in the regulation of non-muscle or smooth muscle myosin RLC phosphorylation during contractile stimulation in this tissue. We find that ROCK regulates airway smooth muscle contraction by collaborating with the serine-threonine kinase Pak to activate Cdc42, leading to the activation of N-WASp, which transmits signals from cdc42 to the Arp2/3 complex for the nucleation of actin filaments. Our results show that the kinase activity of ROCK is required for the activation of Pak. Activated Pak then catalyzes paxillin phosphorylation on Ser273 and coupling of the GIT1-βPIX-Pak signaling module to paxillin, which activates the GEF activity βPIX towards cdc42 (Zhang *et al.*, 2016). ROCK is therefore an upstream mediator of N-WASp activation and actin polymerization. Our results demonstrate a novel molecular function for ROCK in the regulation of Pak and cdc42 activation that is critical for the processes of actin polymerization and contractility in airway smooth muscle.

The role of ROCK in the regulation of myosin light chain phosphatase is well established, and this role is important in regulating the contractility of a number of smooth muscle tissues (Amano *et al.*, 1996; Kimura *et al.*, 1996; Somlyo & Somlyo, 2003; Puetz *et al.*, 2009). Myosin light chain phosphatase, with its regulatory subunit, myosin phosphatase target subunit 1 (MYPT1), can modulate the Ca^{2+}-dependent phosphorylation of myosin RLC by myosin light chain kinase, which is essential for smooth muscle contraction (Pfitzer, 2001; Ito *et al.*, 2004; Khromov *et al.*, 2009; Eto & Kitazawa, 2017). MYPT1 is a known substrate for ROCK; ROCK can phosphorylate MYPT1 on Thr696 or Thr853 (Eto & Kitazawa, 2017). Biochemical studies suggest that while phosphorylation of MYPT1 at Thr696 causes the inactivation of myosin phosphatase and enhances myosin RLC phosphorylation, MYPT1 phosphorylation at the Thr853 site does not inactivate myosin phosphatase (Eto & Kitazawa, 2017) . Studies in bladder and airway smooth muscles have confirmed that MYPT1 Thr853 phosphorylation increases in response to ROCK activation (Qiao *et al.*, 2014; Gao *et al.*, 2017). However, consistent with the biochemical observations, these studies found no role for MYPT Thr853 phosphorylation in regulating myosin RLC phosphorylation and force development in either tissue.

In the current study, we found that expression of the inactive ROCK mutant ROCK121G or the treatment of tissues with the ROCK inhibitor H-1152P inhibited MYPT1 phosphorylation on Thr853 in the airway smooth muscle tissues in response to contractile

stimulation, indicating that these treatments were effective at inhibiting ROCK. However, while ROCK inhibition suppressed tension development in response to ACh stimulation, it had had no effect on myosin RLC phosphorylation (Fig. 1). These results indicate that the role of ROCK in tension development in airway smooth muscle does not result from an inhibitory effect on myosin light chain phosphatase. Our results are consistent with previous studies indicating that MYPT1 Thr853 phosphorylation does not regulate myosin RLC phosphorylation or tension development in airway smooth muscle, and that MYPT1 Thr853 phosphorylation by ROCK does not regulate myosin phosphatase activity (Eto & Kitazawa, 2017; Gao *et al.*, 2017). These observations suggest that ROCK regulates tension development in airway smooth muscle by a different mechanism.

Actin polymerization plays a critical role in tension generation in airway smooth muscle and in other smooth muscle tissues (Mehta & Gunst, 1999; Zhang *et al.*, 2005; Corteling *et al.*, 2007; Rembold *et al.*, 2007; Gunst & Zhang, 2008; Kim *et al.*, 2008; Hill & Meininger, 2012; Walsh & Cole, 2013; Hill & Meininger, 2016; Hong *et al.*, 2016). In airway smooth muscle, cortical actin polymerization may enable the transmission of force generated by crossbridge cycling within the contractile apparatus to membrane adhesion sites that connect smooth muscle cells to the extracellular matrix (Zhang *et al.*, 2005; Gunst & Zhang, 2008; Zhang & Gunst, 2008). We found that ROCK inhibition had a profound inhibitory effect on stimulus-induced actin polymerization during the contractile stimulation of airway smooth muscle under conditions in which no effect on myosin RLC phosphorylation was detected (Figs. 1, 2). ROCK inhibition also profoundly suppressed the activation of N-WASp and prevented the activation of cdc42 (Fig. 8). Thus, our evidence suggests that ROCK acts to regulate upstream processes critical to stimulus-induced N-WASp activation and actin polymerization.

Contractile stimulation triggers the recruitment of inactive cytoplasmic adhesome proteins to membrane adhesion junctions, where they form signaling complexes that regulate cytoskeletal dynamics and actin polymerization (Gunst & Zhang, 2008; Zhang & Gunst, 2008; Zhang *et al.*, 2012; Zhang *et al.*, 2015; Zhang *et al.*, 2016; Zhang & Gunst, 2017). In airway smooth muscle, the recruitment of proteins to the membrane is mediated by NM myosin II that is localized in the cortical region of the airway smooth muscle cell (Zhang & Gunst, 2017). Contractile stimulation triggers the polymerization of NM myosin II filaments through a process that is dependent on RhoA activation: RhoA regulates NM myosin II assembly in part by regulating the phosphorylation of NM myosin RLC (Zhang & Gunst, 2017). We therefore

explored the possibility that ROCK might act as a RhoA effector to regulate the NM myosin RLC phosphorylation, NM myosin filament assembly and/or NM myosin II activation. Our results provided no evidence for a role for ROCK in NM myosin RLC phosphorylation or in NM myosin II filament assembly in response to ACh (Fig. 3). We also evaluated the effect of ROCK inhibition on the recruitment of inactive adhesome proteins to membrane adhesion complexes, as this process is mediated by NM myosin II. Using PLA, we found no effect of ROCK inhibition on the ACh-stimulated recruitment of paxillin-vinculin complexes to the membrane or on the binding of vinculin to talin within adhesome complexes (Fig 4). We conclude that ROCK does not regulate NM myosin activation or adhesome complex assembly during contractile stimulation, and that ROCK must be acting to regulate actin polymerization at a step that is downstream of adhesome complex assembly, but upstream activation of cdc42 and N-WASp activation (Fig. 9).

Paxillin localized within membrane adhesome complexes can undergo phosphorylation on Tyrosine 31 and 118 by FAK, which enables it to couple to N-WASp via the adaptor protein Crk II (Parsons *et al.*, 1994; Petit *et al.*, 2000; Tang *et al.*, 2003; Tang *et al.*, 2005). Paxillin also undergoes phosphorylation on Ser273 by Pak, which is necessary for the coupling of GIT1 to paxillin and the localization of the GIT1-βPIX-Pak signaling module within adhesomes (Nayal *et al.*, 2006; Frank & Hansen, 2008; Zhang *et al.*, 2016). We found that ROCK inhibition had no effect on paxillin Tyr118 phosphorylation, but that ROCK inhibition suppressed paxillin phosphorylation on Ser273 (Fig. 5). Consistent with these results, the coupling of paxillin to GIT1 was also prevented by ROCK inhibition (Fig. 6).

As the phosphorylation of paxillin on Ser273 is catalyzed by Pak (Nayal *et al.*, 2006; Zhang *et al.*, 2016), we investigated the possibility that ROCK contributes to the regulation of Pak activation. Our results show that ROCK inactivation suppresses the ACh-induced activation of Pak (Fig. 7). As we are not aware of previous evidence in any cell type demonstrating a role for ROCK in regulating Pak activation, we performed co-immunoprecipitation analysis to determine whether contractile stimulation triggers the interaction of ROCK with Pak. ROCK and Pak co-precipitated in immunocomplexes from tissues that were stimulated with ACh, but not in unstimulated tissues or in tissues in which ROCK activity was inhibited (Fig.7). This provides additional evidence that ROCK mediates Pak activation during the contractile stimulation of this tissue. Pak may directly facilitate Pak activation by regulating its kinase activity, perhaps by catalyzing its phosphorylation, or ROCK might indirectly facilitate Pak activation through a scaffolding function. The GIT1-

βPIX-Pak signaling module activates cdc42 in this tissue through the GEF activity of βPIX (Zhang *et al.*, 2016), we therefore determined the effect of ROCK inactivation on cdc42 activation. ROCK inhibition prevented the activation of cdc42 in response to ACh stimulation, which is consistent with our evidence for its role in regulating Pak activation and paxillin Ser273 phosphorylation (Fig.8).

In summary, our evidence supports the conclusion that ROCK regulates airway smooth muscle contractility by regulating the activation of Pak within membrane adhesome complexes. This facilitates paxillin Ser273 phosphorylation and the coupling of the GIT1-βPIX -Pak signaling module to paxillin, which is required for the activation of the small GTPase cdc42. As activation of the actin polymerization initiator, N-WASp, is dependent on the GTPase activity of cdc42, ROCK regulates actin polymerization and airway smooth muscle contractility through it role in regulating Pak activity. These findings document a novel role for ROCK in the regulation of airway smooth muscle contractility that is distinct from its previously described role in regulating myosin light chain phosphatase and myosin RLC phosphorylation.

A molecular function for ROCK in the regulation of Pak and activation of the GIT1-βPIX -Pak complex has not been previously described in smooth muscle or and other cell types. The GIT1-βPIX -Pak signaling module is important for processes involved in cell migration (Nayal *et al.*, 2006; Frank & Hansen, 2008; Guilluy *et al.*, 2011). Thus, it is possible that the molecular function of ROCK in the regulation of Pak activation described in our study also plays an important role in processes involved in the migration of other cell types.

Our studies have previously documented the critical functions of the large multiprotein complexes (adhesomes) that reside at the sites of mechanical coupling between smooth muscle cells and their matrix environment within intact muscle tissues (Gunst & Zhang, 2008; Zhang & Gunst, 2008; Zhang *et al.*, 2012; Zhang *et al.*, 2015; Zhang & Gunst, 2017). Adhesome complexes not only mediate cellular pathways that regulate smooth muscle contractility, but they are critical for other cellular processes that allow muscle tissues to sense and respond to changes in the properties of their surrounding milieu (Gunst & Zhang, 2008; Wu *et al.*, 2008; Zhang & Gunst, 2008; Desai *et al.*, 2011; Wu *et al.*, 2016). Our current observations provide further evidence that the process of signal transduction initiated by the contractile stimulation of smooth muscle tissues involves multiple parallel cellular processes that must be coordinated to generate a functional physiological response. The role

of signaling proteins in the pathways that regulate the activation of smooth muscle myosin and crossbridge cycling have been extensively studied. While the activation of contractile proteins is critical to tension development, other cellular processes that regulate cytoskeletal assembly and organization are clearly also essential for the physiologic responses of muscle tissues. The role of ROCK in regulating the activity of adhesome signal modules may also be fundamental to the processes of signal transduction in response to extracellular stimuli that regulate non-contractile functions smooth muscle tissues; and this function may also be applicable to a variety of other of contractile and motile cell types.

References

Amano M, Ito M, Kimura K, Fukata Y, Chihara K, Nakano T, Matsuura Y & Kaibuchi K. (1996). Phosphorylation and activation of myosin by Rho-associated kinase (Rho-kinase). *J Biol Chem* **271,** 20246-20249.

Amano M, Nakayama M & Kaibuchi K. (2010). Rho-kinase/ROCK: A key regulator of the cytoskeleton and cell polarity. *Cytoskeleton (Hoboken)* **67,** 545-554.

Amin E, Dubey BN, Zhang SC, Gremer L, Dvorsky R, Moll JM, Taha MS, Nagel-Steger L, Piekorz RP, Somlyo AV & Ahmadian MR. (2013). Rho-kinase: regulation, (dys)function, and inhibition. *Biol Chem* **394,** 1399-1410.

Beach JR & Hammer JA, 3rd. (2015). Myosin II isoform co-assembly and differential regulation in mammalian systems. *Exp Cell Res* **334,** 2-9.

Beach JR, Shao L, Remmert K, Li D, Betzig E & Hammer JA, 3rd. (2014). Nonmuscle myosin II isoforms coassemble in living cells. *Curr Biol* **24,** 1160-1166.

Corteling RL, Brett SE, Yin H, Zheng XL, Walsh MP & Welsh DG. (2007). The functional consequence of RhoA knockdown by RNA interference in rat cerebral arteries. *Am J Physiol Heart Circ Physiol* **293,** H440-H447.

Croft DR, Sahai E, Mavria G, Li S, Tsai J, Lee WM, Marshall CJ & Olson MF. (2004). Conditional ROCK activation in vivo induces tumor cell dissemination and angiogenesis. *Cancer Res* **64,** 8994-9001.

Desai LP, Wu Y, Tepper RS & Gunst SJ. (2011). Mechanical stimuli and IL-13 interact at integrin adhesion complexes to regulate expression of smooth muscle myosin heavy chain in airway smooth muscle tissue. *Am J Physiol Lung Cell Mol Physiol* **301,** L275-L284.

Eto M & Kitazawa T. (2017). Diversity and plasticity in signaling pathways that regulate smooth muscle responsiveness: Paradigms and paradoxes for the myosin phosphatase, the master regulator of smooth muscle contraction. *J Smooth Muscle Res* **53,** 1-19.

Frank SR & Hansen SH. (2008). The PIX-GIT complex: a G protein signaling cassette in control of cell shape. *Semin Cell Dev Biol* **19,** 234-244.

Gao N, Tsai MH, Chang AN, He W, Chen CP, Zhu M, Kamm KE & Stull JT. (2017). Physiological vs. pharmacological signalling to myosin phosphorylation in airway smooth muscle. *J Physiol* **595,** 6231-6247.

Gosens R, Schaafsma D, Nelemans SA & Halayko AJ. (2006). Rho-kinase as a drug target for the treatment of airway hyperrespon-siveness in asthma. *Mini Rev Med Chem* **6,** 339-348.

Grassie ME, Moffat LD, Walsh MP & MacDonald JA. (2011). The myosin phosphatase targeting protein (MYPT) family: a regulated mechanism for achieving substrate specificity of the catalytic subunit of protein phosphatase type 1delta. *Arch Biochem Biophys* **510,** 147-159.

Guilluy C, Garcia-Mata R & Burridge K. (2011). Rho protein crosstalk: another social network? *Trends Cell Biol* **21,** 718-726.

Gunst SJ & Zhang W. (2008). Actin cytoskeletal dynamics in smooth muscle: a new paradigm for the regulation of smooth muscle contraction. *AJP - Cell Physiology* **295,** C576-C587.

Herrera AM, Martinez EC & Seow CY. (2004). Electron microscopic study of actin polymerization in airway smooth muscle. *Am J Physiol Lung Cell Mol Physiol* **286,** L1161-L1168.

Higgs HN & Pollard TD. (2000). Activation by Cdc42 and PIP(2) of Wiskott-Aldrich syndrome protein (WASp) stimulates actin nucleation by Arp2/3 complex. *J Cell Biol* **150,** 1311-1320.

Hill MA & Meininger GA. (2012). Arteriolar vascular smooth muscle cells: mechanotransducers in a complex environment. *Int J Biochem Cell Biol* **44,** 1505-1510.

Hill MA & Meininger GA. (2016). Small artery mechanobiology: Roles of cellular and non-cellular elements. *Microcirculation* **23,** 611-613.

Hong K, Zhao G, Hong Z, Sun Z, Yang Y, Clifford PS, Davis MJ, Meininger GA & Hill MA. (2016). Mechanical activation of angiotensin II type 1 receptors causes actin remodelling and myogenic responsiveness in skeletal muscle arterioles. *J Physiol* **594,** 7027-7047.

Huang Y, Day RN & Gunst SJ. (2014). Vinculin phosphorylation at Tyr1065 regulates vinculin conformation and tension development in airway smooth muscle tissues. *J Biol Chem* **289,** 3677-3688.

Huang Y, Zhang W & Gunst SJ. (2011). Activation of vinculin induced by cholinergic stimulation regulates contraction of tracheal smooth muscle tissue. *J Biol Chem* **286,** 3630-3644.

Ikebe M, Hartshorne DJ & Elzinga M. (1986). Identification, phosphorylation, and dephosphorylation of a second site for myosin light chain kinase on the 20,000-dalton light chain of smooth muscle myosin. *J Biol Chem* **261,** 36-39.

Ikenoya M, Hidaka H, Hosoya T, Suzuki M, Yamamoto N & Sasaki Y. (2002). Inhibition of rho-kinase-induced myristoylated alanine-rich C kinase substrate (MARCKS) phosphorylation in human neuronal cells by H-1152, a novel and specific Rho-kinase inhibitor. *J Neurochem* **81,** 9-16.

Ito M, Nakano T, Erdodi F & Hartshorne DJ. (2004). Myosin phosphatase: structure, regulation and function. *Mol Cell Biochem* **259,** 197-209.

Khromov A, Choudhury N, Stevenson AS, Somlyo AV & Eto M. (2009). Phosphorylation-dependent autoinhibition of myosin light chain phosphatase accounts for Ca2+ sensitization force of smooth muscle contraction. *J Biol Chem* **284,** 21569-21579.

Kim HR, Gallant C, Leavis PC, Gunst SJ & Morgan KG. (2008). Cytoskeletal Remodeling in Differentiated Vascular Smooth Muscle is Actin Isoform-Dependent and Stimulus-Dependent. *AJP - Cell Physiology* **295,** C768-C778.

Kimura K, Ito M, Amano M, Chihara K, Fukata Y, Nakafuku M, Yamamori b, Feng J, Nakano T, Okawa K, Iwamatsu A & Kaibuchi K. (1996). Regulation of myosin phosphatase by Rho and Rho-associated kinase (Rho-kinase). *Science* **273,** 245-248.

Kume H. (2008). RhoA/Rho-kinase as a therapeutic target in asthma. *Curr Med Chem* **15,** 2876-2885.

Lan B, Deng L, Donovan GM, Chin LY, Syyong HT, Wang L, Zhang J, Pascoe CD, Norris BA, Liu JC, Swyngedouw NE, Banaem SM, Pare PD & Seow CY. (2015). Force maintenance and myosin filament assembly regulated by Rho-kinase in airway smooth muscle. *Am J Physiol Lung Cell Mol Physiol* **308,** L1-10.

Leung T, Chen XQ, Manser E & Lim L. (1996). The p160 RhoA-binding kinase ROK alpha is a member of a kinase family and is involved in the reorganization of the cytoskeleton. *Mol Cell Biol* **16,** 5313-5327.

Liu C, Zuo J & Janssen LJ. (2006). Regulation of airway smooth muscle RhoA/ROCK activities by cholinergic and bronchodilator stimuli. *Eur Respir J* **28,** 703-711.

Maekawa M, Ishizaki T, Boku S, Watanabe N, Fujita A, Iwamatsu A, Obinata T, Ohashi K, Mizuno K & Narumiya S. (1999). Signaling from Rho to the actin cytoskeleton through protein kinases ROCK and LIM-kinase. *Science* **285,** 895-898.

Matsui T, Amano M, Yamamoto T, Chihara K, Nakafuku M, Ito M, Nakano T, Okawa K, Iwamatsu A & Kaibuchi K. (1996). Rho-associated kinase, a novel serine/threonine kinase, as a putative target for small GTP binding protein Rho. *Embo j* **15,** 2208-2216.

Mehta D & Gunst SJ. (1999). Actin polymerization stimulated by contractile activation regulates force development in canine tracheal smooth muscle. *J Physiol* **519 Pt 3,** 829-840.

Nayal A, Webb DJ, Brown CM, Schaefer EM, Vicente-Manzanares M & Horwitz AR. (2006). Paxillin phosphorylation at Ser273 localizes a GIT1-PIX-PAK complex and regulates adhesion and protrusion dynamics. *J Cell Biol* **173,** 587-589.

Opazo Saez A, Zhang W, Wu Y, Turner CE, Tang DD & Gunst SJ. (2004). Tension development during contractile stimulation of smooth muscle requires recruitment of paxillin and vinculin to the membrane. *Am J Physiol Cell Physiol* **286,** C433-C447.

Oude Weernink PA, Schulte P, Guo Y, Wetzel J, Amano M, Kaibuchi K, Haverland S, Voss M, Schmidt M, Mayr GW & Jakobs KH. (2000). Stimulation of phosphatidylinositol-4-phosphate 5-kinase by Rho-kinase. *J Biol Chem* **275,** 10168-10174.

Parsons JT, Schaller MD, Hildebrand J, Leu TH, Richardson A & Otey C. (1994). Focal adhesion kinase: structure and signalling. *J Cell Sci Suppl* **18,** 109-113.

Petit V, Boyer B, Lentz D, Turner CE, Thiery JP & Valles A. (2000). Phosphorylation of tyrosine residues 31 and 118 on paxillin regulates cell migration through an association with CRK in NBT-II cells. *J Cell Biol* **148,** 957-970.

Pfitzer G. (2001). Invited review: regulation of myosin phosphorylation in smooth muscle. *J Appl Physiol* **91,** 497-503.

Puetz S, Lubomirov LT & Pfitzer G. (2009). Regulation of smooth muscle contraction by small GTPases. *Physiology (Bethesda)* **24,** 342-356.

Qiao YN, He WQ, Chen CP, Zhang CH, Zhao W, Wang P, Zhang L, Wu YZ, Yang X, Peng YJ, Gao JM, Kamm KE, Stull JT & Zhu MS. (2014). Myosin phosphatase target subunit 1 (MYPT1) regulates the contraction and relaxation of vascular smooth muscle and maintains blood pressure. *J Biol Chem* **289,** 22512-22523.

Rembold CM, Tejani AD, Ripley ML & Han S. (2007). Paxillin phosphorylation, actin polymerization, noise temperature, and the sustained phase of swine carotid artery contraction. *Am J Physiol Cell Physiol* **293,** C993-1002.

Rohatgi R, Ho HY & Kirschner MW. (2000). Mechanism of N-WASP activation by CDC42 and phosphatidylinositol 4, 5-bisphosphate. *J Cell Biol* **150,** 1299-1310.

Rohatgi R, Ma L, Miki H, Lopez M, Kirchhausen T, Takenawa T & Kirschner MW. (1999). The interaction between N-WASP and the Arp2/3 complex links Cdc42-dependent signals to actin assembly. *Cell* **97,** 221-231.

Somlyo AP & Somlyo AV. (2003). Ca2+ sensitivity of smooth muscle and nonmuscle myosin II: modulated by G proteins, kinases, and myosin phosphatase. *Physiol Rev* **83,** 1325-1358.

Somlyo AP & Somlyo AV. (2004). Signal transduction through the RhoA/Rho-kinase pathway in smooth muscle. *J Muscle Res Cell Motil* **25,** 613-615.

Tang DD & Gunst SJ. (2004). The small GTPase Cdc42 regulates actin polymerization and tension development during contractile stimulation of smooth muscle. *J Biol Chem* **279,** 51722-51728.

Tang DD, Turner CE & Gunst SJ. (2003). Expression of non-phosphorylatable paxillin mutants in canine tracheal smooth muscle inhibits tension development. *J Physiol* **553,** 21-35.

Tang DD, Zhang W & Gunst SJ. (2005). The adapter protein CrkII regulates neuronal Wiskott-Aldrich syndrome protein, actin polymerization, and tension development during contractile stimulation of smooth muscle. *J Biol Chem* **280,** 23380-23389.

Walsh MP & Cole WC. (2013). The role of actin filament dynamics in the myogenic response of cerebral resistance arteries. *J Cereb Blood Flow Metab* **33,** 1-12.

Worthylake RA & Burridge K. (2003). RhoA and ROCK promote migration by limiting membrane protrusions. *J Biol Chem* **278,** 13578-13584.

Wu X, Suetsugu S, Cooper LA, Takenawa T & Guan JL. (2004). Focal Adhesion Kinase Regulation of N-WASP Subcellular Localization and Function. *J Biol Chem* **279,** 9565-9576.

Wu Y, Huang Y & Gunst SJ. (2016). Focal adhesion kinase (FAK) and mechanical stimulation negatively regulate the transition of airway smooth muscle tissues to a synthetic phenotype. *Am J Physiol Lung Cell Mol Physiol* **311,** L893-l902.

Wu Y, Huang Y, Herring BP & Gunst SJ. (2008). Integrin-linked kinase regulates smooth muscle differentiation marker gene expression in airway tissue. *Am J Physiol Lung Cell Mol Physiol* **295,** L988-L997.

Yoshii A, Iizuka K, Dobashi K, Horie T, Harada T, Nakazawa T & Mori M. (1999). Relaxation of contracted rabbit tracheal and human bronchial smooth muscle by Y-27632 through inhibition of Ca2+ sensitization. *Am J Respir Cell Mol Biol* **20,** 1190-1200.

Yu JS, Chen WJ, Ni MH, Chan WH & Yang SD. (1998). Identification of the regulatory autophosphorylation site of autophosphorylation-dependent protein kinase (auto-kinase).

Evidence that auto-kinase belongs to a member of the p21-activated kinase family. *Biochem J* **334 (Pt 1),** 121-131.

Zenke FT, King CC, Bohl BP & Bokoch GM. (1999). Identification of a central phosphorylation site in p21-activated kinase regulating autoinhibition and kinase activity. *J Biol Chem* **274,** 32565-32573.

Zhang W, Du L & Gunst SJ. (2010). The effects of the small GTPase RhoA on the muscarinic contraction of airway smooth muscle result from its role in regulating actin polymerization. *Am J Physiol Cell Physiol* **299,** C298-C306.

Zhang W & Gunst SJ. (2008). Interactions of airway smooth muscle cells with their tissue matrix: implications for contraction. *Proc Am Thorac Soc* **5,** 32-39.

Zhang W & Gunst SJ. (2017). Non-muscle (NM) myosin heavy chain phosphorylation regulates the formation of NM myosin filaments, adhesome assembly and smooth muscle contraction. *J Physiol* **595,** 4279-4300.

Zhang W, Huang Y & Gunst SJ. (2012). The small GTPase RhoA regulates the contraction of smooth muscle tissues by catalyzing the assembly of cytoskeletal signaling complexes at membrane adhesion sites. *J Biol Chem* **287,** 33996-34008.

Zhang W, Huang Y & Gunst SJ. (2016). p21-Activated kinase (Pak) regulates airway smooth muscle contraction by regulating paxillin complexes that mediate actin polymerization. *J Physiol* **594,** 4879-4900.

Zhang W, Huang Y, Wu Y & Gunst SJ. (2015). A novel role for RhoA GTPase in the regulation of airway smooth muscle contraction. *Can J Physiol Pharmacol* **93,** 129-136.

Zhang W, Wu Y, Du L, Tang DD & Gunst SJ. (2005). Activation of the Arp2/3 complex by N-WASp is required for actin polymerization and contraction in smooth muscle. *Am J Physiol Cell Physiol* **288,** C1145-C1160.

ADDITIONAL INFORMATION

Conflicts of Interest. The authors declare that they have no conflicts of interest with the contents of this article.

Author Contributions: WZ designed the experiments with SJG, conducted the experiments, analyzed the results, and wrote the paper with SJG. BPB designed the experiments with SJG,

conducted experiments, and analyzed the results. SJG conceived of the idea for the project, designed the experiments with BPB and WZ, supervised the data analysis and wrote the paper with WZ. All authors approved the final version of the manuscript and agree to be accountable for all aspects of the work. All persons designated as authors qualify for authorship, and all those who qualify for authorship are listed.

FIGURE LEGENDS

Figure 1. ROCK inactivation inhibits ACh stimulated tension development but not myosin RLC phosphorylation in tracheal smooth muscle tissues. A. Contractile force in response to ACh before and after tissues were transfected with plasmids encoding WT ROCK, ROCK K121G or no plasmids (Sham). ROCK K121G mutant (n=7) or treatment with H-1152P (n=7) significantly inhibited ACh-induced tension development. Values for force were calculated as a percentage of pretreatment maximal force in response to 10^{-5} M ACh, which was approximately 10 g for most tissues. B. *Upper,* The expression of myc-ROCK1 K121G and WT ROCK1 in transfected tissues was confirmed by dual immunofluorescence against ROCK1 (*green band*) and the myc epitope (*red band*). *Lower,* Immunoblot for MYPT1 phosphorylation in tissue extracts by dual immunofluorescence against MYPT1 (*red band*) and P-Thr853 MYPT (*green band*). MYPT1 Ab and P-Thr853 MYPT Ab reactive proteins overlay to a single band (*yellow band*). C. The phosphorylation of MYPT1 increased with ACh stimulation and was inhibited by expression of ROCK K121G or by treatment with H-1152P. D. Unphosphorylated and phosphorylated smooth muscle 20 kD myosin RLCs were separated by urea gel electrophoresis and quantified as the ratio of phosphorylated myosin RLCs to total myosin RLCs in each sample. Inhibition of ROCK activation with ROCK K121G (n=5) or H-1152P (n=8) did not affect the increase in myosin RLC phosphorylation in response to ACh stimulation (*Left*). All values are mean ± SEM. *Significant difference between treatment groups ($p < 0.05$). ns, not significantly different.
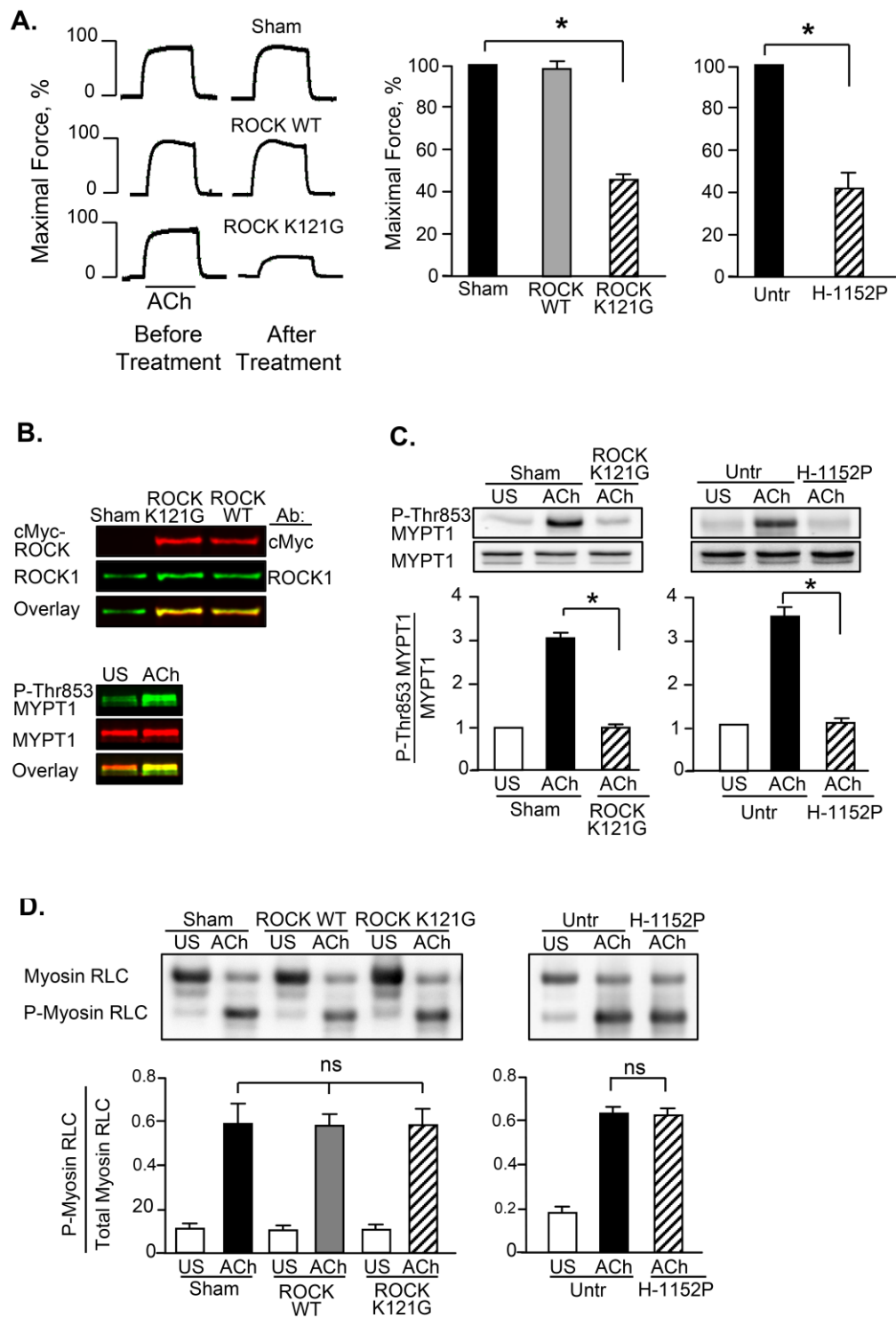
Figure 1

Figure 2. ROCK regulates actin polymerization and N-WASp phosphorylation in response to ACh stimulation in tracheal smooth muscle tissues. Immunoblot of soluble G-actin (globular) and insoluble F-actin (filamentous) in fractions from extracts of unstimulated (US) or ACh stimulated muscle tissues. Ratios of F-actin to G-actin were determined by quantitating F and G actin in extracts from each muscle strip. Inhibition of ROCK activation with ROCK K121G (n=5) or H-1152P (n=8) prevented the increase in F-actin/G-actin ratio in response to ACh stimulation. Values are means ± SEM. * Significant difference between treatments, p< 0.05.
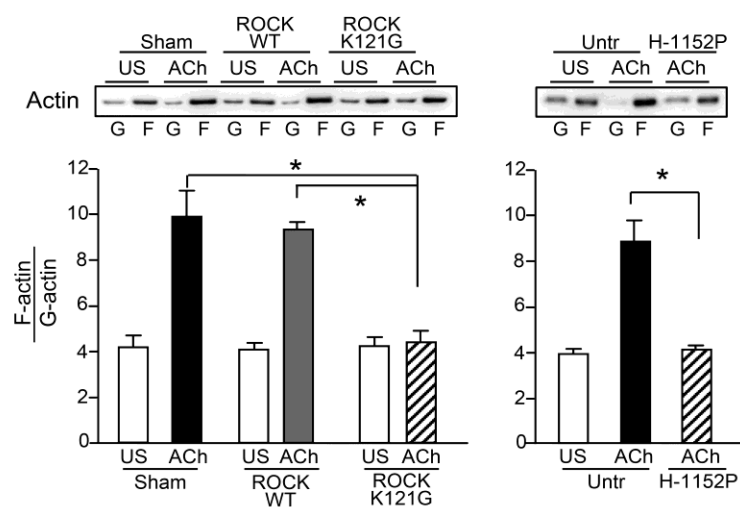

Figure 2

Figure 3. ROCK does not regulate NM myosin RLC phosphorylation in response to ACh stimulation in tracheal smooth muscle tissues. A. Representative immunoblots of myosin RLCs from unstimulated (US) and ACh-stimulated muscle tissues. Myosin RLCs were separated by two-dimensional electrophoresis and immunoblotted for myosin RLC. Unphosphorylated SM myosin RLC migrated to spot 1, mono-phosphorylated SM myosin RLC migrated to spot 2, and di-phosphorylated SM myosin RLC migrated to spot 3. Unphosphorylated and phosphorylated NM myosin RLC migrated to spots 3 and 4 respectively. Expression of ROCK K121G did not significantly affect the increase of NM myosin RLC phosphorylation in response to ACh stimulation (See methods for quantitative analysis) (n=7, p> 0.05). B. Immunoblot of NM myosin IIA from soluble (S) and cytoskeletal (pellet, P) fractions of extracts from tracheal smooth muscle tissues treated with ROCK K121G or Sham-treated, and stimulated with ACh or unstimulated (US). The ratio of NM myosin II in the cytoskeletal (P) versus soluble (S) fractions increased in response to 5 min stimulation with 10^{-5} M ACh in both sham and ROCK K121G-treated tissues. The expression of ROCK K121G did not significantly affect the movement of NM myosin into the pellet fraction in response to stimulation with 10^{-5} M ACh (n=5). C. Interactions between NM myosin IIA and NM myosin IIB isoforms in unstimulated (US) and ACh-stimulated freshly dissociated smooth muscle cells assessed by *in situ* proximity ligation assay (PLA). Images show PLA fluorescence alone and merged with phase contrast. ACh stimulation of either Sham-treated or ROCK K121G treated tissues resulted in a significant increase in the number of NM myosin IIA and IIB complexes at the cell membrane (Sham: US, n=21; ACh, n=27; ROCK K121G: US, n=21; ACh, n=26). The number of ACh-stimulated NM myosin IIA and IIB complexes was not significantly different in Sham-treated tissues or in tissues expressing ROCK K121G. Values are means ± SEM. ns, not significantly different.
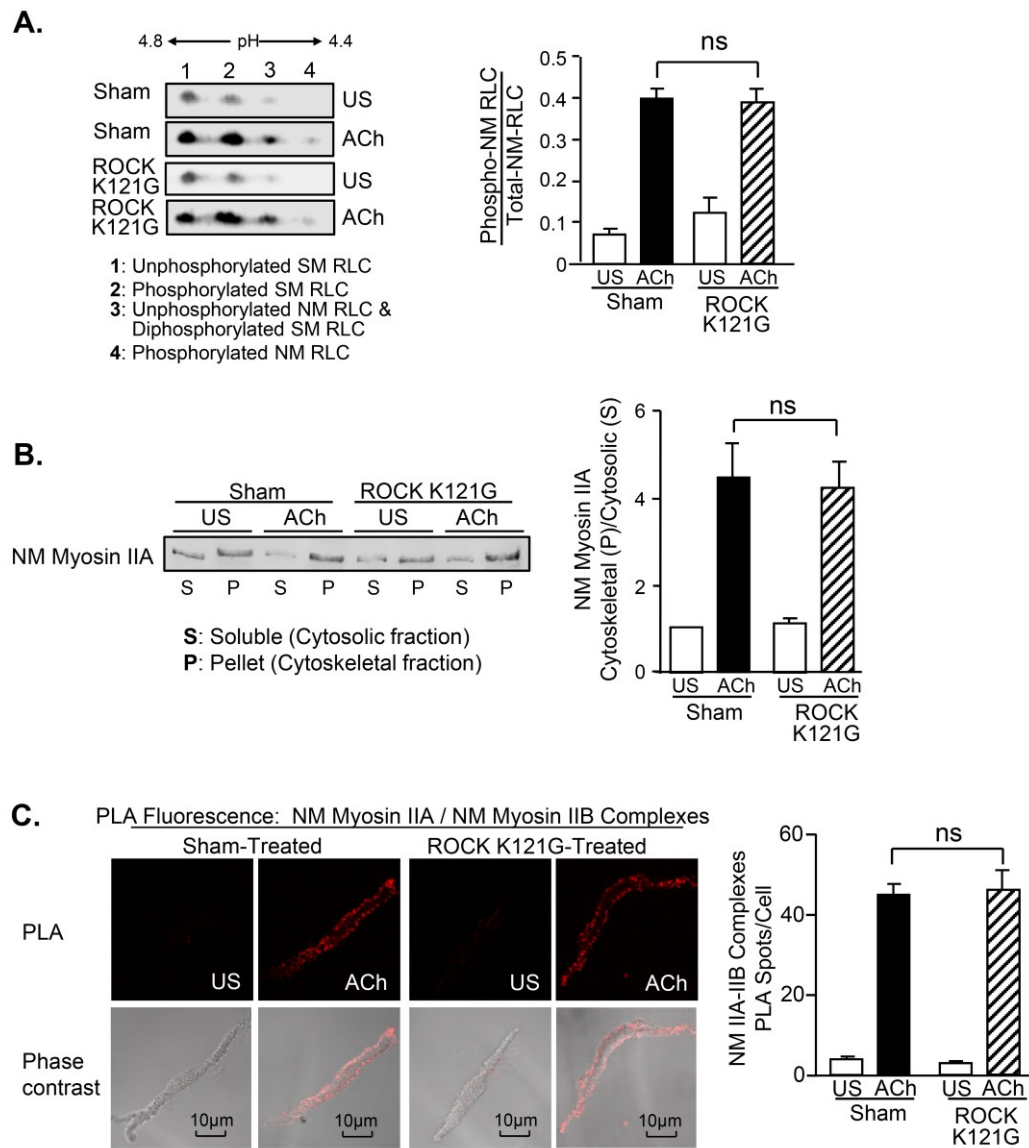
Figure 3

A.

4.8 ←—— pH ——→ 4.4

	1	2	3	4	
Sham					US
Sham					ACh
ROCK K121G					US
ROCK K121G					ACh

1: Unphosphorylated SM RLC
2: Phosphorylated SM RLC
3: Unphosphorylated NM RLC & Diphosphorylated SM RLC
4: Phosphorylated NM RLC

$\frac{\text{Phospho-NM RLC}}{\text{Total-NM-RLC}}$

ns

US   ACh   US   ACh
Sham   ROCK K121G

B.

Sham   ROCK K121G
US   ACh   US   ACh

NM Myosin IIA

S P   S P   S P   S P

S: Soluble (Cytosolic fraction)
P: Pellet (Cytoskeletal fraction)

NM Myosin IIA Cytoskeletal (P)/Cytosolic (S)

ns

US   ACh   US   ACh
Sham   ROCK K121G

C.

PLA Fluorescence: NM Myosin IIA / NM Myosin IIB Complexes

	Sham-Treated		ROCK K121G-Treated	
PLA	US	ACh	US	ACh
Phase contrast	10µm	10µm	10µm	10µm

NM IIA-IIB Complexes PLA Spots/Cell

ns

US   ACh   US   ACh
Sham   ROCK K121G

Figure 4. ROCK does not regulate the assembly of adhesome complexes in response to ACh stimulation in tracheal smooth muscle tissues. Interactions between paxillin and vinculin (A) or vinculin and talin (B) in unstimulated (US) and ACh-stimulated freshly dissociated smooth muscle cells assessed by *in situ* proximity ligation assay (PLA). Images show PLA fluorescence alone and merged with phase contrast. A. Paxillin-vinculin complexes are distributed throughout the cytoplasm of unstimulated cells. ACh stimulates the localization of paxillin-vinculin complexes to the membrane in all cells whether or not they were treated with H-1152P. Cells shown are representative of results in cells dissociated from tissues from 3 separate experiments (No inhibitor: US, n=14; ACh, n=17; H-1152P: US, n=14; ACh, n=14). B. Very few interactions between vinculin and talin were observed in unstimulated cells. ACh stimulation of tracheal smooth muscle cells resulted in a significant increase in the number of PLA spots at the cell membrane indicating interactions between vinculin and talin whether or not tissues were treated with H-1152P (Untreated: US, n=18; ACh, n=24). H-1152P treatment did not significantly affect the increase in the number of PLA spots at the cell membrane (US, n=20; ACh, n=21). Cells dissociated from tissues obtained from 3 separate experiments. Values are means ± SEM. ns, not significantly different.
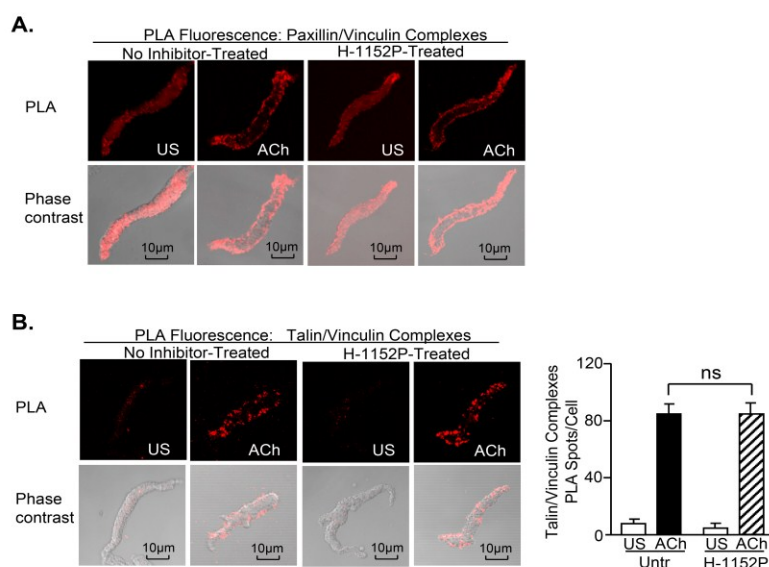
Figure 4

Figure 5. ROCK regulates the phosphorylation of paxillin on Ser273 in response to stimulation with ACh in tracheal smooth muscle tissues. Paxillin Tyr118 phosphorylation and paxillin Ser273 phosphorylation were measured in unstimulated (US) or ACh stimulated tracheal smooth muscle tissues. A. ROCK inactivation by the ROCK K121G mutant significantly inhibited ACh induced paxillin Ser273 phosphorylation, but it did not significantly affect paxillin Tyr118 phosphorylation (n=5). B. ROCK inhibition by H-1152P treatment significantly inhibited ACh induced paxillin Ser273 phosphorylation, but it did not significantly affect paxillin Tyr118 phosphorylation (n=11). Values are means ± SEM.* Significant difference between treatments, $p < 0.05$.

Figure 5
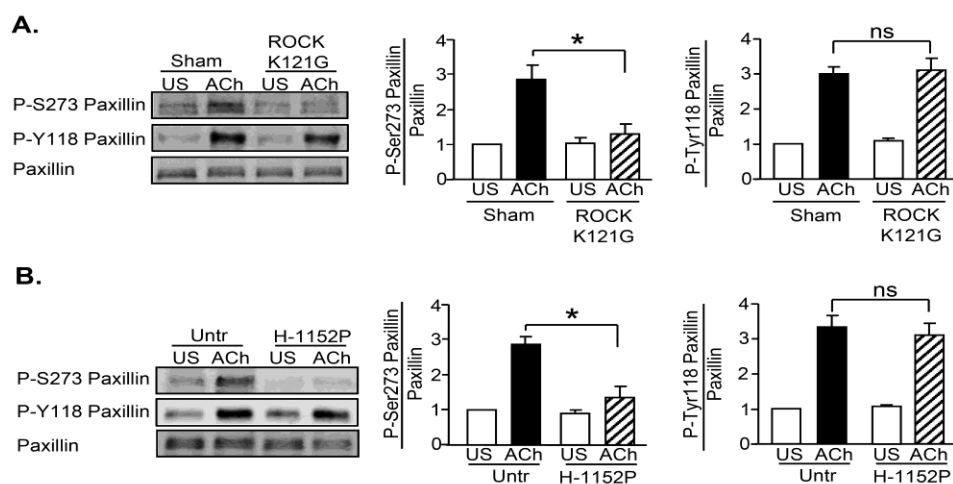
Figure 6. ROCK regulates the interaction of paxillin and GIT1 at the cell membrane during contractile stimulation. *In situ* proximity ligation assay (PLA) shows the interaction of paxillin and GIT1 in freshly dissociated differentiated canine tracheal smooth muscle cells. PLA fluorescence is shown alone and merged with phase contrast images for each cell. A. ACh stimulated a significant increase in the number of interactions between paxillin and GIT1 in Sham treated tissues. In cells from ROCK K121G treated tissues, the mean number of PLA spots was very small and did not increase significantly with ACh-stimulation (Sham: US, n=42; ACh, n=38; ROCK K121G: US, n=26; ACh, n=36). Cells dissociated from tissues obtained from 3 separate experiments. B. ACh stimulation of tracheal smooth muscle cells resulted in a significant increase in the number of PLA spots at the cell membrane indicating interactions between paxillin and GIT1 (US, n=13; ACh, n=18). H-1152P treatment significantly inhibited the number of ACh-induced interactions between paxillin and GIT1 (US, n=13; ACh, n=17). Cells dissociated from tissues obtained from 2 separate experiments. Values are means ± SEM.* Significant difference between treatments, $p < 0.05$.
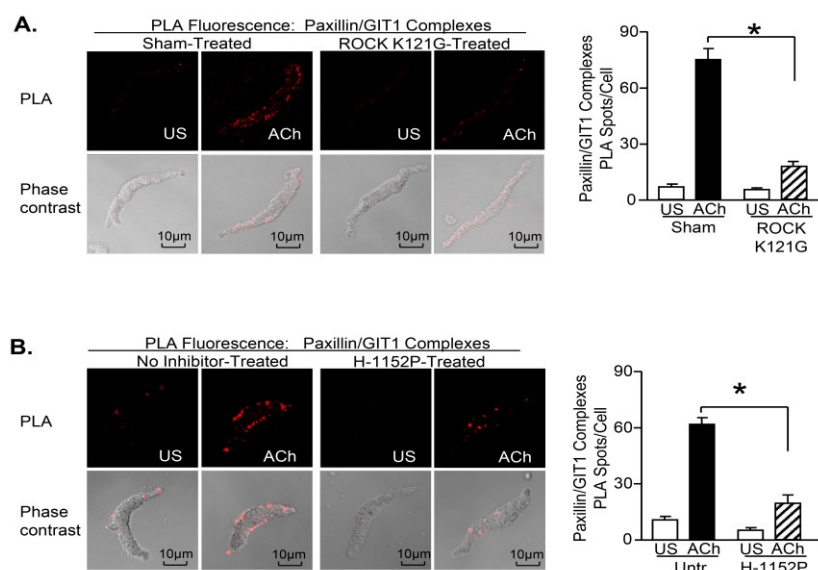
Figure 6

Figure 7. ROCK regulates the activation of p21-activated kinase (Pak) in response to ACh stimulation in airway smooth muscle tissues. A. Pak Thr423 phosphorylation was measured by immunoblot in extracts of muscle tissues transfected with ROCK K121G or sham-treated. Expression of ROCK K121G (n=6) or treatment with H-1152P (n=6) significantly inhibited ACh-induced Pak Thr423 phosphorylation. B. Pak1 (*left*) or ROCK1 (*right*) was immunoprecipitated from extracts of canine tracheal smooth muscle tissues stimulated for 5 min with ACh or unstimulated (US). Tissues were treated with H-1152P to inhibit ROCK activation or not treated. Co-immunoprecipitation of ROCK1 with PAK1 increased after contractile stimulation with ACh in tissues not treated with inhibitor, and was significantly inhibited in tissues treated with H-1152P (n=5 (*left*) or 3 (*right*).
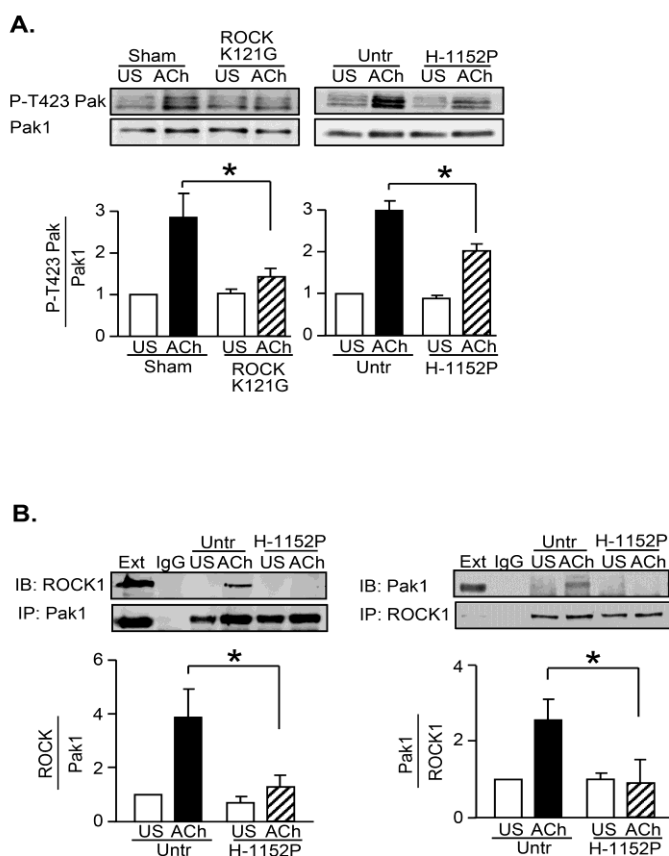
Figure 7

Figure 8. ROCK regulates the activation of cdc42 and N-WASp in response to ACh stimulation in airway smooth muscle tissues. *A.* Activated cdc42 (cdc42-GTP) was affinity-precipitated from extracts of unstimulated and ACh-stimulated muscle strips, and the amount of activated cdc42 precipitated from each extract was quantified by immunoblot. Activated cdc42 was significantly higher in extracts from 10-M ACh stimulated sham-treated tissues than from ACh stimulated tissues expressing ROCK K121G (n=3). H-1152P also inhibited the activation of cdc42 (n=3). *B.* N-WASp Tyr256 phosphorylation measured by immunoblot in extracts of muscle tissues. Expression of ROCK K121G (n=5) or ROCK inhibition with H-1152P (n=5) significantly inhibited ACh-induced N-WASp phosphorylation in tracheal smooth muscle tissues. Values are means ± SEM.* Significant difference between treatments, p< 0.05.
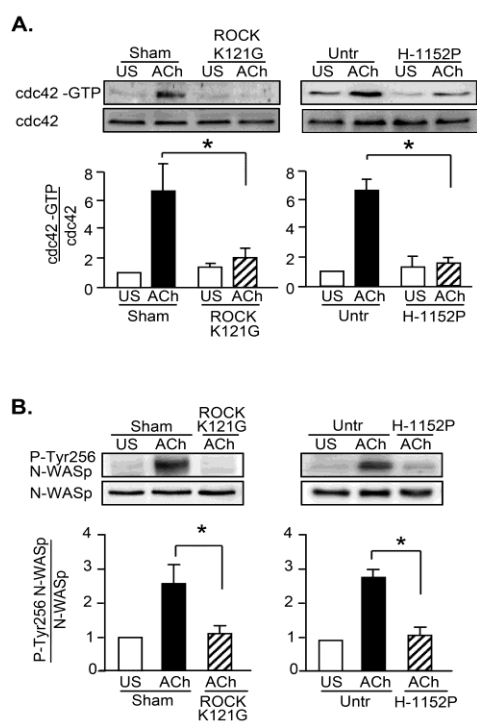
Figure 8

Figure 9. Proposed mechanism for the role of ROCK in the regulation of Pak activation and the assembly of a multiprotein adhesome complex in airway smooth muscle. A,B. Molecular mechanisms for the regulation of actin polymerization by ROCK in response to contractile stimulation: Contractile stimulation activates RhoA GTPase, which directly catalyzes the assembly and activation of NM myosin filaments that mediate the recruitment of paxillin/vinculin complexes and FAK to membrane adhesion sites (*blue arrows*). Paxillin is phosphorylated on Tyr 31 and Tyr118, which enables its coupling to N-WASp via the adaptor protein CrkII. Cdc42 binds to the CRIB domain of N-WASp. RhoA also activates ROCK, which regulates the activation of Pak (*red arrows*). Pak then catalyzes the phosphorylation of paxillin on Ser273. Paxillin 273 phosphorylation promotes its interaction with the GIT1-βPIX-PAK complex by enabling the binding of paxillin to GIT1. βPIX acts as a GEF to regulate the activation of cdc42. Activated cdc42 catalyzes the activation of N-WASp, which leads to actin polymerization by the Arp2/3 complex. **B.** Tension development requires concurrent activation of cellular processes that catalyze actin polymerization and crossbridge cycling. The polymerization of actin at the cortex of the cell and the fortification of the adhesome junctions facilitates the transmission of tension generated by contractile apparatus to the extracellular matrix when crossbridge cycling is activated by smooth muscle myosin RLC phosphorylation.

Figure 9

A.

B.
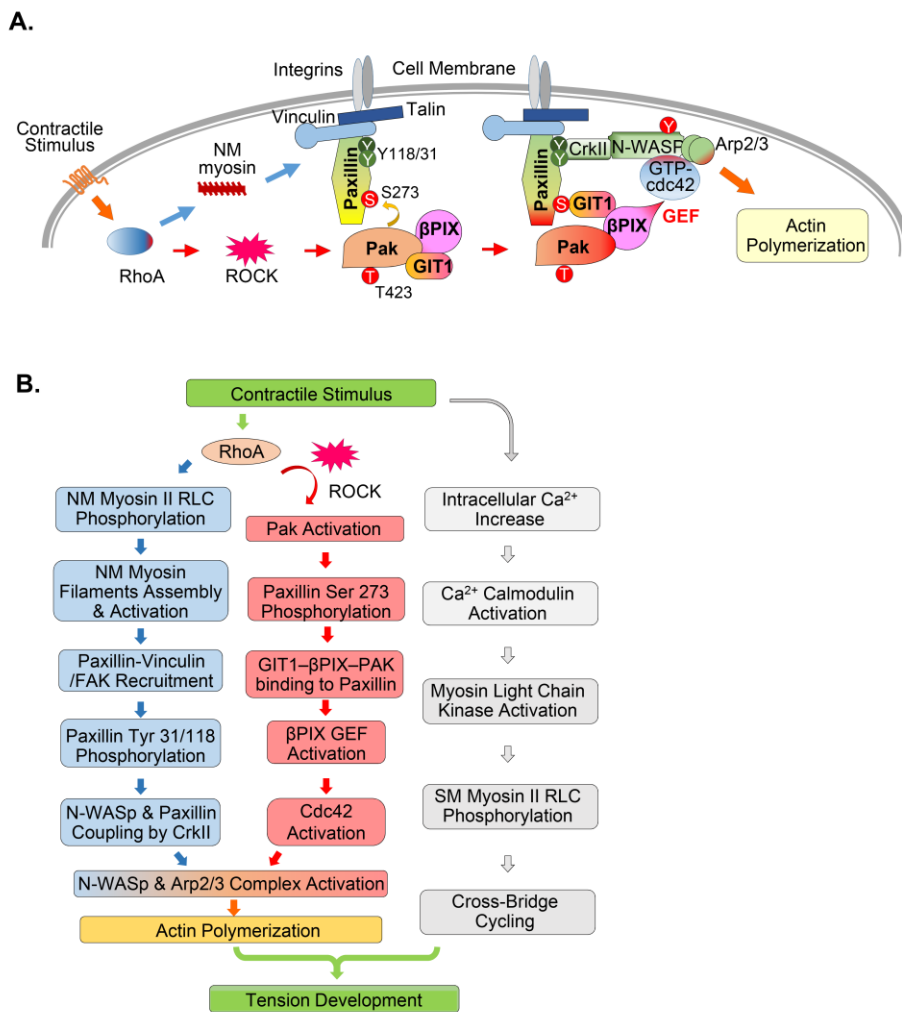
Wenwu Zhang was trained as a cardiothoracic surgeon in China. He moved to Indianapolis, Indiana, USA in 2000 and obtained his PhD in Physiology from Indiana University in 2004. He joined the laboratory of Dr. Susan Gunst at Indiana University School of Medicine, where he pursues research directed at the mechanisms by which cytoskeletal proteins regulate smooth muscle contractility and phenotype in response to physiologic stimuli or changes in environmental conditions. His studies have described several novel mechanisms by which adhesion junction signaling complexes regulate actin polymerization and the dynamics of cytoskeletal organization to mediate the responses of smooth muscle to physiologic stimuli.